A MODEL FOR BINDER GAS GENERATION AND TRANSPORT IN SAND CORES AND MOLDS

Andrei Starobin[1], C.W. Hirt[1], D. Goettsch[2]
[1]Flow Science, Inc.; 683A Harkle Road; Santa Fe, New Mexico, 87505, USA
[2]GM Powertrain, 777 Joslyn Ave; Pontiac, Michigan, 48340, USA

Keywords: Computational fluid dynamics; Fixed-mesh method; Thermal degradation of binders; Core Gas Flow; Casting

Abstract

Gas defects are often found in sand-cast parts that arise from gas generated by thermal decomposition of the sand binder. Typically, these defects occur with sand cores that have not been adequately vented. A new computational model has been developed that predicts the generation of decomposed binder gas and its transport within cores. The binder gas is treated as compressible to account for poor venting scenarios and for transport across core regions of steep temperature gradients. The model considers true molding geometry and actual core venting locations and can be used to predict the amount of gas that would enter liquid metal from any location on the surface of the core.

Overview

The making of resin-bonded sand castings has made great strides in quality over its long history. Even so, there remain some process-related defects that are not fully understood and can cause quality issues. For instance, chemical binders in the sand can produce gas when heated by the molten metal and if this gas is not vented adequately, the gas may flow into the metal resulting in a gas porosity defect. This is most likely with cores that form thin interior features of castings that heat up quickly and have long venting paths. In addition to the core geometry, the composition of the binder may play an important role as well.

Two major types of binders are used in core making practice: resin-based organic binders and inorganic binders such as sodium silicate [9]. The organic binders are either thermosetting, or cured at room temperature with an aid of a catalyst. These are favored in many applications due to their complete degradation even at aluminum casting temperatures and for the ease of subsequent sand shake out. The presented core gas model is developed with these binders in mind, but can be extended to inorganic binders if appropriate data on their decomposition is available.

The thermal degradation of a resin-based binder can be experimentally characterized in two ways: by measuring the mass loss of the binder over time at a fixed heating rate [3,4, 13], or by measuring the amounts and types of volatile and condensable decomposition products over time and over a range of temperatures [5,7, 10, 11]. A reliable model for core gas flow which would predict core gas pressures requires both types of data.

The experimental techniques that quantify the amount of binder gas can be broadly classified as displacement in type [7, 10], or as pressure based methods [11]. In the former, collected gas displaces oil in a tank with the back of the tank vented to the ambient pressure. In the latter, the gas is collected in a fixed volume apparatus and the gas pressure is measured. In both cases the

collection lines are kept at an elevated temperature to prevent condensation of the volatile components which contribute to core pressure. Also, in both cases the standard volumetric rate of the product gas is reported over time.

The data obtained by the pressure based method was used to calibrate the proposed binder decomposition model. The model assumes that the binder converts completely into gas. The gas is thought to be ideal and of fixed composition with the gas constant, R_g. The gas constant is deduced from the total collected standard volume, V_{std}, and the initial mass of the binder, m_b:

$$R_{cg} = \frac{p_{std}}{T_{std}} \frac{V_{std}}{m_b} \tag{1}$$

The major factors contributing to core gas pressure are described by Campbell [1]. Briefly, the hot product gas forms over a range of temperatures estimated in this work to be roughly between 500 and 700 K for resin-based binders. The gas then flows toward the vents through porous sand with an associated pressure loss. The sand porosity can be as high as 40% [9]. Venting either occurs naturally at the back of the mold, or is introduced by drilling through the mold halves to the core print locations. The vent locations are near room temperature during the casting pour.

Three regions of flow can be identified: the high temperature decomposition region, the flow through a steep thermal gradient which can be as high as 10^5 K/m on the core surfaces in iron castings, and finally near-isothermal flow away from core surface to the vents.

In what follows, we formulate the binder decomposition and mass transport model through porous cores or molds. We then show that a simple two-parameter decomposition model adequately captures volume evolution data from a typical polyurethane cold-box (PUCB) calibration core immersed in iron. The model is the then used to compute thermal expansion driven air flow out of a spherical core which was studied in recent experiments [7]. Finally, we present some validation results for vented and unvented aluminum engine block PUCB jacket cores studied at a General Motors Research Foundry. The simulations demonstrate how our core-gas model can be used concurrently with an existing simulation program [12] which is routinely used to study mould filling and casting freezing.

The Core Gas Model

The microscopic velocity of the core gas, $\vec{u}_{cg}$, is governed by the equation for flow in porous media:

$$\vec{u}_{cg} = -\frac{K}{\mu} \nabla p_{cg}, \tag{2}$$

where K is the intrinsic sand permeability found to be approximately 10^{-10} m^2 in room temperature air flow experiments [11], μ is core gas viscosity and p_{cg} is the core gas pressure. Both the macroscopic inertial terms and the Forchheimer term are found to be small for the typical conditions of the core gas flow and are not included in Equation (2). Furthermore, the possible compositional and temperature dependence of the gas viscosity is not accounted for in the model.

The density of the core gas is governed by the mass transport equation:

$$\frac{\partial \rho_{cg}}{\partial t} + \nabla \bullet \left(\rho_{cg} \vec{u}_{cg} \right) = -\frac{d\rho_b}{dt},$$

$$(3)$$

where ρ_{cg} and ρ_b are microscopic core gas and macroscopic core binder densities. The core gas is compressible. For example, even in the absence of gas sources there can be a thermal expansion and flow of the initial air in the core as the core heats up. Furthermore, while the pressures in the cores are expected to be a few psi above ambient and are effectively limited by the surrounding metal pressure, the temperature variations from core surface to the vents are factors of two suggesting significant contraction of core gas during flow.

The density transport equation, Equation (3), must be numerically solved with an implicit coupling to the velocity equation to insure computational stability at reasonable time-step sizes. This is achieved by using a variant of the Implicit Continuous-fluid Eulerian (ICE) method [6].

The core gas density is further constrained by the ideal gas law which should describe well the binder product gas, especially at high temperatures:

$$p_{cg} = R_{cg} \rho_{cg} T \qquad (4)$$

The gas constant R_{cg} is computed using Equation (1), while the temperature of the gas is assumed to be the local core temperature. This is a good approximation because of the high heat content of the solid core material compared to that of the gas.

Since it is assumed that the core and gas temperatures are equal, and the core temperature T is already computed by a heat transfer solver, the ideal gas law can be used to compute gas pressure when its density is given or vice versa. In the present model the core gas density is evaluated from a transport Equation (3).

The conversion of the solid binder to gas is described by an Arrhenius relationship in accord with a number of previous thermal decomposition studies on polymers [3, 4, 13]:

$$\frac{d\rho_b}{dt} = -\rho_b C_b \exp\left(-\frac{E_b}{RT} \right),$$

$$(5)$$

Where ρ_b is the solid binder density, C_b is an empirical reaction rate constant, E_b is a component binding energy, R is the universal gas constant and T is the core temperature. Study [4] is particularly relevant since the two reaction constants were determined for pyrolisis of polyurethane resins at different heating rates. The two constants are 134 kJ/mol and $4.25 \, 10^{10} \, s^{-1}$ and the reaction order is close to one hence the simple form of Equation (5). The highest heating rate probed in this pyrolisis study was only 0.3 deg/sec, while at the core surface in iron immersions the heating rate is as high as 80 deg/sec. However, at this point this is the best data available and we use it for the simulations described below.

Using the exponential Arrhenius rate for binder decomposition can introduce some undesirable computational effects. For example, for the decomposition law of Equation (5) with the listed reaction constants, most of the binder loss happens between 645 and 700 K. Given the steep temperature gradient of about 10^5 K/m at the core surface, even at mesh resolutions of 2 mm the change in temperature between the surface core cell and its neighbor in the core interior is larger than the decomposition zone width. Thus at this mesh resolution the source may exhibit an unphysical oscillatory behavior associated with the discrete size of the computational elements. To alleviate this problem simple subdivision scheme is used in each computational cell. In the

sub-cells solid binder density is stored, while the sub-cell temperature is obtained through linear interpolation of the coarse temperature field.

Two more simplifying assumptions are made at this point. First, no gas is allowed to condense within the core. For most practical cases, condensation, if it occurs, is not likely to significantly affect the early gas pressures that are the principal source for gas related casting defects. Second, the possible endo- or exo-thermic effects of pyrolitic binder decomposition are ignored.

Because the core-gas model is used concurrently with a mold filling model [12], it is possible that gas flow in cores may become sufficiently fast to limit the computational time-step size (by the Courant stability condition for an explicit advection approximation) to a value smaller than what is needed for the filling simulation, resulting in longer calculation times. To counter this possibility, a sub-time-stepping scheme has been incorporated into the core-gas model. This is possible because the model is coupled to the metal filling simulation through boundary conditions (see below). If it is found that the time-step size for the core-gas model must be smaller than that for the filling simulation, then the time-step size for the core-gas computations is reduced to a stable value. The smaller value is always some integer fraction of the original value so that the gas computations can be repeated for that integer number of steps to bring the solution forward to the correct time. The core-gas computations are much faster compared to those for the filling because the gas dynamics is much simpler and the core gas region is only a small portion of a full simulation domain.

Core Boundary Conditions

At boundaries of the core material there may be a flow of gas either in or out of the core. This exchange is treated as a boundary condition for the core-gas model. The passage of gas through the boundary depends on what is located outside the core. For instance, if the core surface is exposed to air, then gas may flow across the boundary in either direction depending on the pressure gradient.

If there is liquid metal at the core surface, then gas is allowed to pass out of the core when its pressure is greater than the pressure of the metal at that location, but no metal is allowed to enter the core. Of course, if the metal has already solidified at the surface of the core, then no gas is allowed to flow across the boundary at that location. In the basic operation of the model, the core gas does not influence metal dynamics. Instead this gas flow is accumulated to identify regions where core gas would percolate into the metal. This option requires the least computational time.

Another boundary condition occurs at print surfaces, that is, where a core surface is in contact with another solid part of the mold. At these surface locations, gas does not normally flow unless channels have been cut into the mold to allow for venting. The core-gas model has an option for allowing venting at print surfaces.

Core Gas Flow in Iron Calibration Experiments

The calibration experiments on small cores were carried out at AlchemCast [11]. A standard size cylindrical core 1.125 inches in diameter and 2 inches long was inserted into an insulating holder and then immersed into the crucible with metal. The size was chosen so that the core gas was sealed at all times with the only escape path at the core top which led into a fixed-volume collection apparatus. The pressure was monitored and subsequently converted into the standard volume.

The left panel of Figure 1 shows the AlchemCast data for a 1.5 wt % PUCB bound core. The gas constant evaluated according to Equation (1) is 357 J/K/mol with a corresponding molar mass of 23 g/mol. This is consistent with the measurements on gas compositions from mold-metal interfaces [5, 9] which indicate that hydrogen, carbon monoxide, methane and carbon dioxide dominate the volatiles (listed in the order of observed abundance).

Overall, the agreement is good, with the peak time captured accurately and the peak rate somewhat underestimated. There is some evidence [5, 9] that composition of collected gas varies from light to heavy during the casting process, the inclusion of which may further improve the agreement between data and simulation. However variable gas composition is beyond the scope of the current model and is a possible future extension.

The right panel of Figure 1 shows the computed decomposition front geometry for the PUCB calibration core at 30 seconds after immersion. The color variable is the solid binder loss rate which is typically ~ 10 kg/m^3/s at, or near the surface in iron immersions. The zone adjacent to the core surface behind the decomposition front contains no intact binder, while the zone adjacent to the vented face has not begun to decompose.
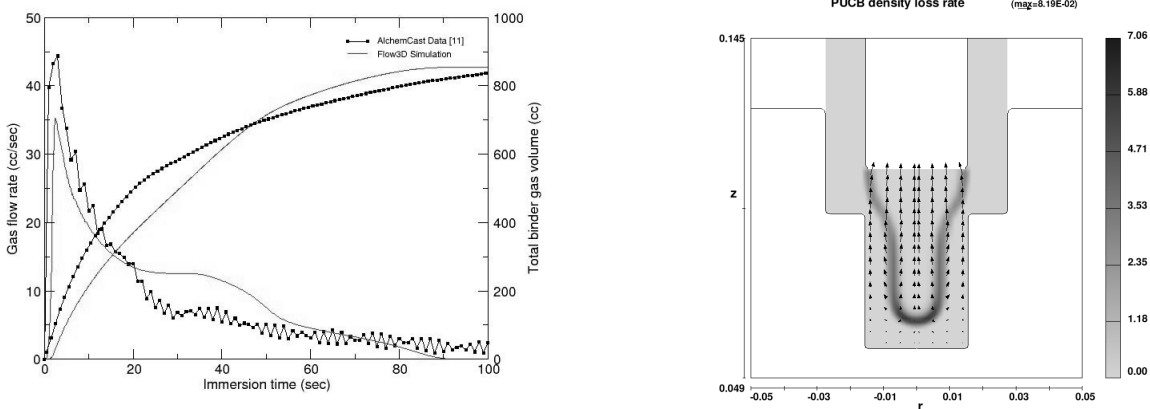
Figure 1. Left panel: Calibration data for a 1.125 in. dia. x 2 in. PUCB core immersed in Iron (2600 F) and results from the FLOW-3D® core gas model. Right panel: The shape of the binder degradation front at 30 seconds after core immersion. The density loss rate has units of kg/m^3/s

Air Flow From A Spherical Core

Recent experiments done at Swecast [7] on small 6 cm diameter spherical cores, show qualitatively similar volumetric rate curves to the one shown in Figure 1. These measurements were performed with the COGAS® apparatus (see [7] for more details) which is based on a displacement technique described above. In [7] the authors point out that the air displaced from the core during immersion is also a contributor to the core pressures. Since our model can be used to study flow of any gas through the porous cores we evaluate the contribution of air to the total volumetric rate signal and the core gas pressure. Our results are summarized in Figure 2. The peak rate of air flow is approximately 0.5 cc/sec and is at about one second after immersion. The peak pressures are only about 5 Pa about the ambient pressure. The experimentally observed peak volumetric rate in [7] is about 20 cc/sec. It is therefore unlikely that air contributes significantly to core pressures in this spherical core, or in larger industrial cores.
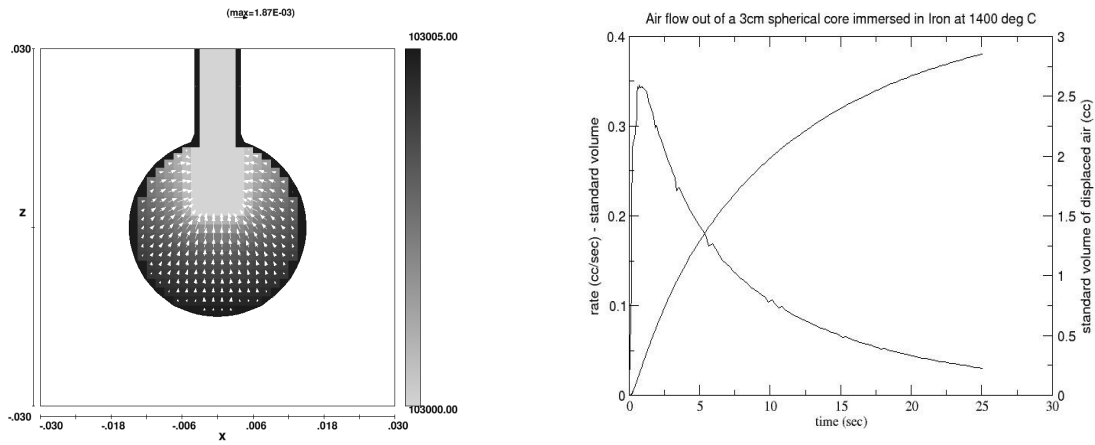
Figure 2. Left: Flow field and pressures in a spherical 6 cm dia. core used in [7] to experimentally monitor volume of binder degradation products. The core is held in place against the immersion tube by buoyancy. Right: Simulated flow rate and total standard volume of core air fluxed from the same core

Flow in Vented and Unvented Engine Block Jacket Cores

Direct observations of core gas bubbles have been made of a vented and an unvented aluminum engine block water jacket core. The jacket and adjoining slab core were placed in an open mold flask, which was bottom filled with 1330F 319 aluminum alloy with a 11 mm/sec vertical velocity (Figure 3). The total fill time was approximately 20 seconds. In the first trial, bubbles were observed through the bulk of the liquid metal as the geometric peaks of the core were submerged. The bubbling stopped when the metal surface reached 75 mm above the top of the cores.

A series of vent holes were formed in the second test core piece. Each core print pad had a 3mm diameter hole, 90 mm long. This left a 60 mm distance from the vent hole to the top of the core where the bubbles were observed in the previous test. No bubbles were observed in the submersion of this vented core.

Figures 3 and 4 summarize the core-gas model results for the two water jacket core submersions. The differences in geometries between the two jacket cores are clearly seen in the panels of Figure 3. The core on the right shows one of three venting holes. Both the gas pressure and the metal pressure in the mold are plotted. It is clear that the vented core is sealed at this point in the fill (at ~ 18 sec). On the other hand the the unvented core also at 18 seconds shows gas blow. The left panel of Figure 3 plots the gas flux at core surface. Loss of gas into the metal is visible in the top portions of the bottom and top halves of the jacket core. The gas blow occurs at sites of lowest local metallostatic head. Additional, desirable gas venting can be seen at prints of the slab core into the mold flask where perfect venting, fixed pressure boundary conditions are set. The same boundary condition is used in the venting holes of the vented jacket core design.
A final observation about the core gas flows in the two cases concerns the peak gas velocity. On average in the vented design the computed velocities are a factor of 2.5 lower.

In Figure 4 we plot the cumulative computed core gas mass rate and the gas blow mass rates in the two designs. The vented core shows a significantly lower gas blow rates during the submersion of the bottom portion of the core and a complete suppression of gas blow past 15 seconds. The computed result is in good agreement with the experimental observations, especially later in the fill. The gradual increase of the gas blow from the unvented core is also in

agreement with foundry observations. A row of bubbles (one per cylinder) was produced after the bottom of the jacket core submerged at about 8 seconds and another row after complete core submersion at approximately 15 seconds.
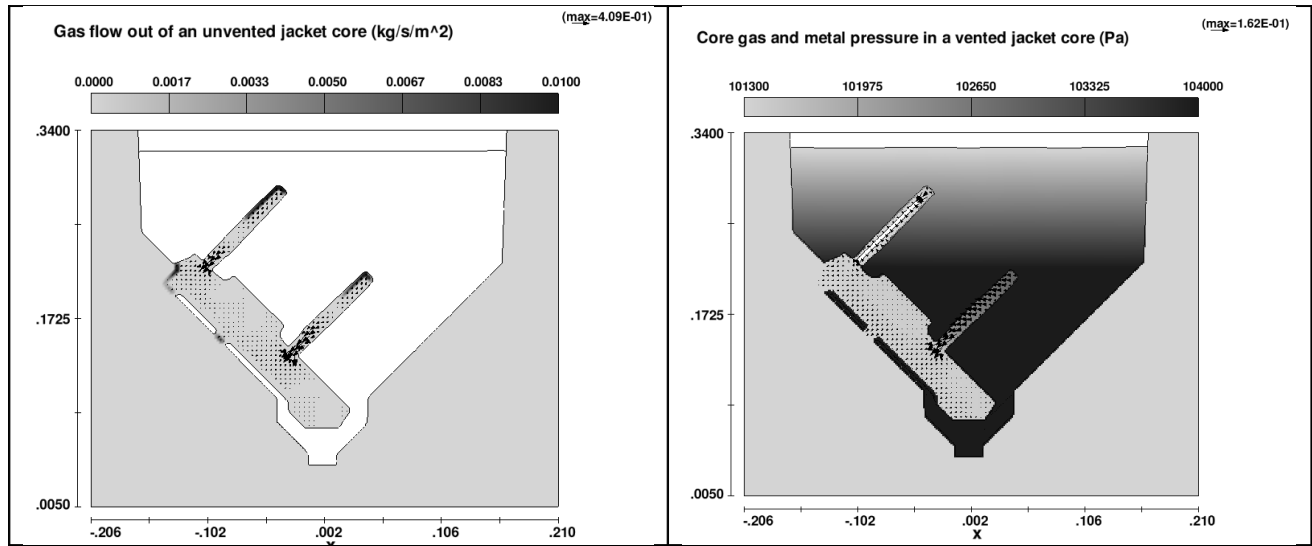
Figure 3: Left panel: Locations and amounts of gas flux from the slab and unvented jacket core. Right panel: Metal pressure and gas pressures in a vented jacket core
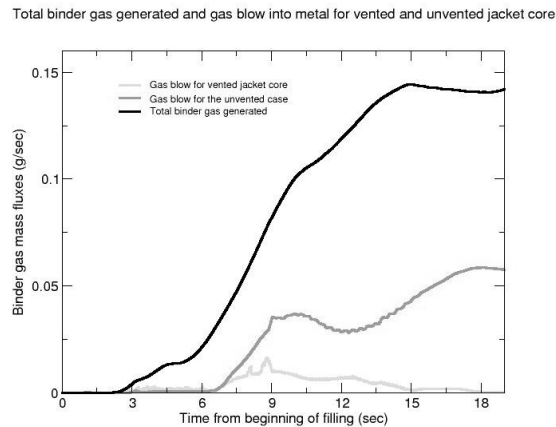
Figure 4: Total binder gas and gas blow into the metal computed for vented and unvented cases.

Conclusions

We have presented a simple, but predictive, model for binder gas generation and transport in sand cores and molds. Future work will focus on extending the model to capture the effect of residual moisture on gas pressures and on validating the existing model for other binder systems such as shell resin. The presented model can be used to capture gas evolution data from simple cores in iron and steel immersions. In more complicated core design situations, the model can be used to evaluate venting strategies, binder content, sands of different permeability and to compare core and molding designs.

Acknowledgements

References

1. J. Campbell, *Castings* (Butterworth-Heinemann, 2000), 105-109

2. Donald A. Nield and Adrian Bejan, *Convection in Porous Media* (Springer, 2006), 5, 39-40

3. Kalayan Annamalai and Ishwar K. Puri, *Combustion Science and Engineering* (CRC Press, 2007), 390-391

4. R. Font et al, "Pyrolysis study of polyurethane", *Journal of Analytical and Applied Pyrolisis*, 58-59, (2001), 63-77

5. W.D. Scott and C.E. Bates, "Decomposition of resin binders and the relationship between gases formed and the casting surface quality", *AFS Transactions*, 1980

6. Harlow, F.H. and Amsden, A.A., "A Numerical Fluid Dynamics Calculation Method for All Flow Speeds," *J. Comput. Phys*. **8**, 197 (1971)

7. J. Orlenius, U. Gotthardsson and A. Dioszegi, *ibid* "Mould and Core Gas Evolution in Grey Iron Castings", *International Journal of Cast Metals Research*, 2008, in press

8. Clive Rogers, "A virtual tool for the manufacture and use of foundry cores and molds", *MCWASP XI*, 2006

9. WD Scott, Hanjun Li, John Griffin, and Charles Bates, "Production and Inspection of Quality Aluminum Castings", in press

10. L. Winardi, R.D. Griffin, H.E. Littleton, J.A. Griffin, "Variables Affecting Gas Evolution Rates and Volumes from Cores in Contact with Molten Metal", *AFS Transactions* **116**, 505-521, 2007

11. AlchemCast LLC, Pelham, Alabama, USA, www.alchemcast.com

12. ***FLOW-3D***® Theory Manual, (Flow Science Inc., Santa Fe, New Mexico, USA, www.flow3d.com , 2008).

13. Lengelle, G., "Thermal Degradation Kinetics and Surface Pyrolysis of Vinyl Polymers", AIAA J., 8(11), 1989-1196, 1970